

Supplemental information

Menke-Hennekam syndrome; delineation of domain-specific subtypes with distinct clinical and DNA methylation profiles

Sadegheh Haghshenas, Hidde J. Bout, Josephine M. Schijns, Michael A. Levy, Jennifer Kerkhof, Pratibha Bhai, Haley McConkey, Zandra A. Jenkins, Ella M. Williams, Benjamin J. Halliday, Sylvia A. Huisman, Peter Lauffer, Vivian de Waard, Laura Witteveen, Siddharth Banka, Angela F. Brady, Elena Galazzi, Julien van Gils, Anna C.E. Hurst, Frank J. Kaiser, Didier Lacombe, Antonio F. Martinez-Monseny, Patricia Fergelot, Fabíola P. Monteiro, Ilaria Parenti, Luca Persani, Fernando Santos-Simarro, Brittany N. Simpson, MKHK Research Consortium, Mariëlle Alders, Stephen P. Robertson, Bekim Sadikovic, and Leonie A. Menke

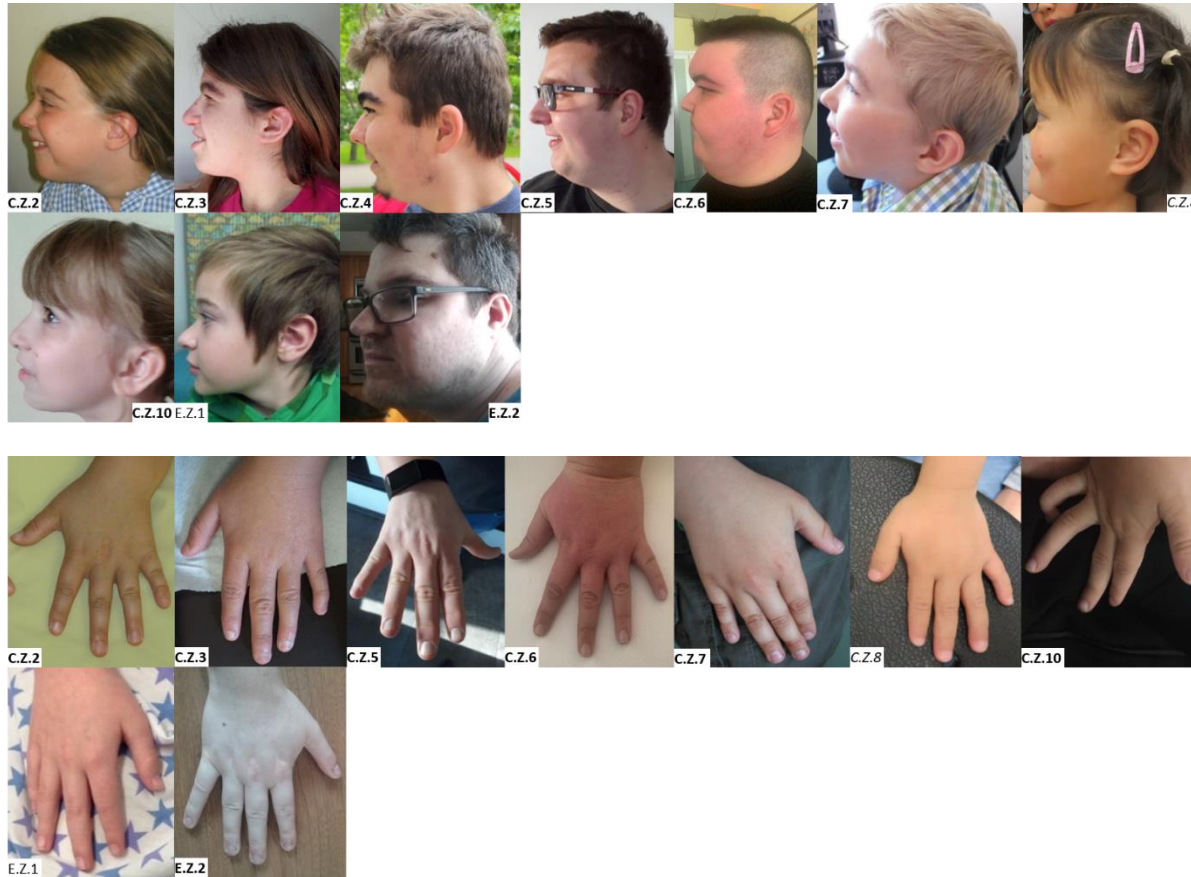
Table of contents

Figure S1. Lateral facial and distal limb morphology of the presently described individuals with a variant in the MKHK region of <i>CREBBP</i> and <i>EP300</i>	2
Table S1. Summary of the 3-step process for the selection of probes	8
Table S2. Morphological characteristics of individuals with a confirmed MKHK methylation profile or epesignature (in ID4) per MKHK subtype.	8
Table S3 (see excel file). Clinical characteristics and morphological features of the presently described individuals with a variant in the MKHK region of <i>CREBBP</i> and <i>EP300</i>	9
Table S4 (see excel file). Genotypes, epesignatures and in silico prediction scores of all presently described individuals with a variant in the MKHK region of <i>CREBBP</i> (NM_004380.2) or <i>EP300</i> (NM_001429.3).....	9
Table S5. List of identified differentially methylated regions.	10
References	12

Figure S1. Lateral facial and distal limb morphology of the presently described individuals with a variant in the MKHK region of *CREBBP* and *EP300*.

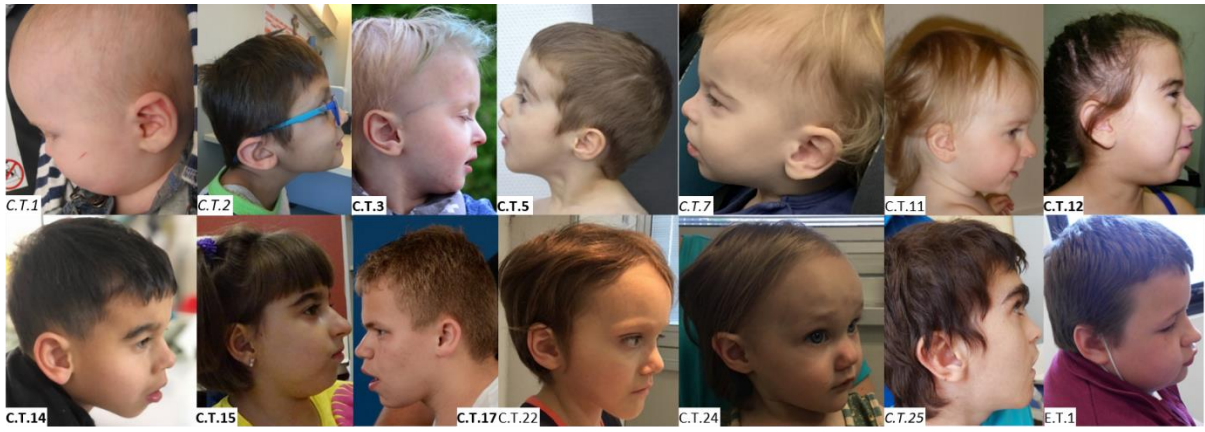
The lateral facial characteristics, the hands and feet of individuals with a variant in (A) the ZZ-domain, (B) TAZ2-domain, (C) ID4, and (D) in between the ZZ and TAZ2-domain (C.ZT.1 en C.ZT.2) and in between TAZ2 and ID4 (C.TI.29). Study numbers are depicted within each photograph reflecting the affected gene (C or E representing *CREBBP* and *EP300*) and domain (Z, T, I, ZT, and TI representing ZZ, TAZ2, ID4, the region between ZZ and TAZ2, and the region between TAZ2 and ID4, respectively) followed by a unique number. The study numbers of individuals with a confirmed MKHK epismutation or methylation profile are displayed in bold, and of individuals who were tested, but in whom no MKHK epismutation or methylation profile was found, in italics. Detailed description of facial and distal limb morphology of all individuals can be found in Table S3.

A





B





C







D



Table S1. Summary of the 3-step process for the selection of probes

Episignature	Number of probes after the first step	Number of probes after the second step	Cut-off value for correlation
MKHK_ZZ	1000	333	0.85
MKHK_TAZ2	900	225	0.75
MKHK_ID4	900	225	0.75

Table S2. Morphological characteristics of individuals with a confirmed MKHK methylation profile or episignature (in ID4) per MKHK subtype.

ZZ, zinc finger ZZ-type; TAZ2, zinc finger TAZ-type; ID4, first α -helix of the fourth intrinsically disordered region of CBP/p300.

	MKHK-ZZ (n=9)	MKHK-TAZ2 (n=14)	MKHK-ID4 (n=21)
Sparse hair	0/9	3/12 (25%)	10/19 (53%)
Prominent forehead	2/9 (22%)	4/13 (31%)	15/20(75%)
Face, square (FS) or flat (FF)	FF 1/9 (11%) FS 1/9 (11%)	FF 1/13 (8%) FS 2/13 (15%)	FF 6/20 (30%) FS 6/20 (30%)
Thick eyebrows	5/9 (56%)	7/13 (54%)	6/21 (29%)
Flared eyebrows	5/9 (56%)	0/13	0/18
Telecanthi (T)/ epicanthi (E)	T 2/9 (22%) E 2/9 (22%)	T 2/14 (14%) E 5/14 (36%)	T 7/21 (33%) E 7/21 (33%)
Palpebral fissures Up (U)- or downslanted (D)	U 0/7 D 1/7 (14%)	U 1/13 (8%) D 2/13 (15%)	U 15/21 (71%) D 0/21
Short palpebral fissures	1/9 (11%)	2/14 (14%)	15/21 (71%)
Ptosis/ Blepharophimosis	4/8 (50%)	5/11 (45%)	15/21 (71%)
Long eyelashes	3/9 (33%)	5/12 (42%)	5/20 (25%)
Ears Low-set (L) / Short (S)	L 0/8 S 0/8	L 2/9 (22%) S 1/9 (11%)	L 6/19 (32%) S 1/19 (5%)
Protruding ears (upper part)	0/9	3/12 (25%)	13/20 (65%)
Overfolded helix	1/8 (13%)	1/11 (9%)	8/19 (42%)
Absent earlobe	0/8	1/11 (9%)	2/19 (10%)
Full cheeks	4/9 (44%)	3/14 (21%)	10/21 (48%)
Malar flattening	0/9	1/12 (8%)	8/18 (44%)
Short nose	2/9 (22%)	2/14 (14%)	11/21 (52%)
Depressed nasal bridge	1/9 (11%)	0/12	9/18 (50%)
Narrow nasal bridge	1/9 (11%)	2/14 (14%)	2/21 (9%)
Depressed nasal ridge	0/9	1/12 (7%)	10/18 (56%)
Broad nasal tip	3/9 (33%)	8/14 (57%)	12/21 (57%)
Short columella	0/8	3/13 (23%)	14/21 (67%)
Anteverted nares	1/9 (11%)	4/14 (29%)	11/21 (52%)
Underdeveloped alae nasi	0/9	1/13 (8%)	1/21 (5%)
Philtrum Short (S)/Long (L)/Deep (D)	S 1/9 (11%) L 1/9 (11%) D 0	S 0/13 L 5/13 (38%) D 1/13 (8%)	S 1/21 (5%) L 13/21 (62%) D 4/21 (19%)
Everted vermilion of upper lip	1/9 (11%)	2/13 (15%)	4/21 (19%)
Thin vermilion of upper lip	5/9 (56%)	4/13 (31%)	6/21 (29%)
High palate	6/7 (86%)	1/10 (10%)	10/17 (59%)
Missing teeth	2/8 (25%)	0/8	3/10 (30%)
Retro- or micrognathia	1/9 (11%)	5/12 (42%)	5/19 (26%)
Ulnar deviation of finger(s)	0/7	0/13	3/20 (15%)
Clinodactyly fifth finger	1/9 (11%)	2/11 (18%)	8/20 (40%)
Tapering fingers	0/6	0/13	2/20 (10%)
Prominent digital pads	0/6	1/8 (13%)	4/15 (27%)
Sandal gap	3/6 (50%)	3/11 (27%)	5/18 (28%)
Overlapping toes	0/6	3/13 (23%)	6/19 (32%)
Halluces Broad (B)/Narrow (N)	0/5	B 2/12 (17%) N 1/12 (8%)	B 3/18 (17%) N 1/18 (6%)
Fibular deviation distal phalanx halluces	0/6	2/12 (17%)	8/20 (40%)
Cutaneous partial syndactyly of toes	0/6	2/12 (17%)	5/18 (28%)

Table S3 (see excel file). Clinical characteristics and morphological features of the presently described individuals with a variant in the MKHK region of *CREBBP* and *EP300*.

The columns of individuals for whom a DNA sample was available are green colored if the diagnosis of the MKHK-subtype was confirmed by episignature testing, and orange colored in case the episignature result did not show any MKHK episignature. ^a Menke et al. 2016¹; ^b Menke et al. 2018²; ^c Angius et al. 2019³; ^d Banka et al. 2019.⁴ ADHD, attention deficit hyperactivity disorder; ASD, autism spectrum disorder; ASDsf: some features of ASD; ASd: atrial septal defect; BMI, body mass index; DMII, diabetes mellitus type 2; Dpt, diopters; eTSH, elevated thyroid stimulating hormone; GE, gastro-esophageal; GHD, growth hormone deficiency; GI, gastrointestinal; G-tube, gastric tube; ID, intellectual disability; IVC, inferior vena cava; LT, low testosterone level; n.a.; not available; OD, right eye; OFC, occipito-frontal circumference; OS, left eye; PDA, patent ductus arteriosus; PEG, percutaneous gastrostomy; PE-tubes, pressure equalizing tubes; PFO, patent foramen ovale; PVL, periventricular leucomalacia; PVS, Pulmonary valve stenosis; RRTI, recurrent respiratory tract infections; RUTI, recurrent urinary tract infections; SDS, standard deviation score; TSH, thyroid stimulating hormone; TVP, tricuspid valve prolapse; VSD, ventricle septal defect; VUR, vesicoureteral reflux.

Table S4 (see excel file). Genotypes, episignatures and in silico prediction scores of all presently described individuals with a variant in the MKHK region of *CREBBP* (NM_004380.2) or *EP300* (NM_001429.3).

ZZ, Zinc-finger ZZ-type; TAZ2, Zinc-finger TAZ-type; ID4, first α -helix of the fourth intrinsically disordered region. ^aGnomAD: number represents how many times the allele was seen in gnomAD (Genome Aggregation Database) with '.' representing not seen, which is slightly different than '0' (seen but filtered out in the final gnomAD population). CADD, Combined Annotation Dependent Depletion; REVEL, Rare Exome Variant Ensemble Learner; SIFT, Sorting Intolerant From Tolerant; PolyPhen, Polymorphism Phenotyping; MPC, 'Missense badness, PolyPhen-2 and Constraint'.

Table S5. List of identified differentially methylated regions.

Chromosome	Start	End	Width	Number of CpGs	Stouffer	Fisher	Maximum difference	Mean difference	Overlapping gene(s)
chr17	40822424	40824241	1818	8	6,98E-77	2,55E-73	0,22913	0,167478	PLEKHH3
chr6	26195488	26197606	2119	8	9,12E-36	1,53E-57	-0,25391	-0,10266	AL031777.2,H3C4
chr6	27858545	27859478	934	6	1,67E-12	1,07E-27	-0,1179	-0,05217	H3C12
chr7	27169136	27171391	2256	21	1,15E-21	3,8E-26	-0,13849	-0,0732	HOXA3,HOXA-AS2,HOXA4,AC004080.6,HOXA-AS3
chr5	42756102	42757815	1714	11	1,26E-13	4,4E-24	-0,1223	-0,05729	CCDC152
chr6	27782126	27783336	1211	6	1,53E-11	1,74E-19	-0,1646	-0,06806	H2AC14,H2BC14
chr17	14205882	14207968	2087	15	1,14E-13	4,14E-19	-0,12428	-0,05383	HS3ST3B1,AC005224.3
chr5	1,5E+08	1,5E+08	1504	10	2,12E-11	1,05E-14	0,116828	0,05455	CAMK2A
chr19	11517079	11517953	875	7	5,16E-07	1,64E-14	0,142259	0,066341	RGL3
chr12	58131345	58133008	1664	9	5,13E-09	5,41E-14	-0,18415	-0,08062	AGAP2,TSPAN31
chr1	1,57E+08	1,57E+08	1268	6	5,09E-12	8,5E-14	-0,14	-0,07838	TTC24
chr6	26224668	26226256	1589	11	8,64E-12	1,97E-13	-0,1307	-0,0787	H3C6
chr12	1641924	1643253	1330	5	2,4E-06	7,74E-12	0,108645	0,056643	WNT5B
chr9	98314632	98315816	1185	6	2,28E-06	4,09E-11	-0,109	-0,05646	
chr1	27675587	27676652	1066	7	3,33E-12	4,22E-11	-0,09359	-0,06941	SYTL1
chr10	70321243	70322874	1632	9	4,52E-06	1,54E-10	-0,11566	-0,05487	TET1
chr19	55660514	55661872	1359	6	7,63E-10	2,9E-10	0,156144	0,086835	TNNT1
chr1	2,36E+08	2,36E+08	785	6	5,47E-09	2,16E-09	0,109219	0,064921	GNG4
chr22	42394048	42395340	1293	11	1,72E-05	4,77E-09	0,115519	0,060151	SEPTIN3,WBP2NL
chr3	1,94E+08	1,94E+08	691	7	2,62E-10	9,62E-09	-0,11353	-0,08543	LINC00887
chr1	11708564	11709491	928	5	5,48E-07	1,85E-08	0,093936	0,051314	FBXO2
chr3	42846594	42847116	523	5	1,09E-06	2,84E-08	-0,11095	-0,05701	AC099329.1,ACKR2
chr3	1,41E+08	1,41E+08	544	6	1,94E-08	2,86E-08	-0,0906	-0,06869	ZBTB38
chr5	79552470	79553606	1137	5	1,92E-08	4,09E-08	-0,11464	-0,069	
chr5	83016630	83017921	1292	11	9,31E-07	4,18E-08	-0,09717	-0,05656	HAPLN1
chr17	46719276	46720386	1111	5	6,27E-08	5,18E-08	0,083397	0,055208	AC103702.2
chr1	2,35E+08	2,35E+08	645	5	1,48E-06	1,18E-07	-0,08859	-0,05036	
chr1	6514605	6516324	1720	5	9,55E-07	2,09E-07	0,096204	0,061211	ESPN
chr2	2,43E+08	2,43E+08	481	5	4,77E-06	8,9E-07	0,081801	0,05709	
chr12	54412506	54413936	1431	8	6,44E-07	2,07E-06	0,099361	0,065565	AC012531.3,HOXC6,HOXC4,AC012531.2,AC012531.1
chr10	21798341	21799395	1055	6	2,59E-06	7,25E-06	-0,09209	-0,06279	
chr17	17109640	17110641	1002	11	6,46E-06	7,78E-06	0,097594	0,066414	MPRIP,PLD6,AC055811.2
chr18	22907319	22908222	904	5	5,9E-05	8,46E-06	-0,12209	-0,07057	ZNF521
chr1	63249197	63249705	509	7	0,002966	9,24E-06	0,113212	0,053852	
chr1	86043795	86044230	436	6	2,59E-05	1,07E-05	-0,09664	-0,06059	DDAH1,AC092807.4,AC092807.3
chr9	35791475	35792382	908	6	9,94E-05	1,16E-05	-0,10736	-0,05536	NPR2
chr15	99408636	99409957	1322	10	2,89E-06	1,37E-05	0,068171	0,053442	IGF1R
chr19	36004632	36005395	764	6	4,15E-05	1,84E-05	0,091674	0,060381	
chr2	1,64E+08	1,64E+08	716	7	1,17E-06	1,95E-05	-0,09102	-0,06841	
chr5	1245669	1246795	1127	6	2,37E-05	2,18E-05	0,094337	0,063162	SLC6A18

chr17	78734663	78735596	934	6	3,78E-05	3,15E-05	0,086993	0,054553	RPTOR
chr1	27683139	27683912	774	7	6,69E-06	3,29E-05	0,064924	0,052358	MAP3K6
chr19	51165207	51165845	639	5	3,59E-05	3,3E-05	0,083174	0,061784	SHANK1
chr11	1769152	1770066	915	9	7,68E-05	3,45E-05	0,079182	0,051487	IFITM10,AC068580.4
chr19	50249464	50249927	464	5	0,000347	4,02E-05	0,12787	0,07806	TSKS
chr4	4763259	4763753	495	7	2,36E-05	6E-05	-0,11503	-0,05714	STX18-AS1
chr1	1289806	1291064	1259	8	5,16E-06	6,02E-05	0,097064	0,058265	MXRA8
chr11	18477153	18478135	983	7	8,57E-05	6,3E-05	0,12583	0,062944	LDHAL6A
chr11	45671208	45672248	1041	5	8,1E-06	6,46E-05	0,087335	0,063194	CHST1
chr12	1,31E+08	1,31E+08	759	7	0,000119	8,38E-05	0,109142	0,054137	STX2
chr9	1,34E+08	1,34E+08	626	5	4,07E-05	9,53E-05	-0,08873	-0,07043	
chr19	49223814	49224454	641	5	3,55E-05	9,9E-05	-0,0969	-0,0565	RASIP1
chr1	6187633	6188136	504	5	2,65E-05	0,000131	0,099593	0,068783	CHD5
chr7	27127448	27128169	722	6	1,99E-05	0,00015	0,067895	0,050098	
chr1	2,44E+08	2,44E+08	1119	5	2,29E-05	0,000164	0,070203	0,052386	ZBTB18
chr17	9549496	9550545	1050	8	0,000162	0,000171	-0,09224	-0,05537	USP43,AC118755.1
chr3	1,84E+08	1,84E+08	634	7	0,000308	0,000185	0,124694	0,051593	CHRD
chr10	75533025	75533431	407	5	0,000418	0,000299	0,102109	0,057383	FUT11
chr1	27718221	27718858	638	5	0,000827	0,0003	0,08923	0,050069	
chr5	2537210	2537834	625	8	0,000111	0,000382	0,087529	0,053924	
chr3	1,6E+08	1,6E+08	480	6	3,71E-05	0,000404	-0,08339	-0,0682	IQCJ-SCHIP1,SCHIP1
chr4	1,75E+08	1,75E+08	208	5	0,00032	0,000408	-0,09371	-0,06334	LINC02269,AC106895.2
chr1	19971709	19972777	1069	8	5,83E-05	0,00061	-0,10402	-0,06221	NBL1,MICOS10-NBL1
chr8	38831681	38832728	1048	6	0,001872	0,001269	-0,07691	-0,05204	HTRA4
chr11	834676	835377	702	5	0,004198	0,001496	0,113156	0,061579	CD151
chr19	50861774	50862121	348	5	0,000291	0,001703	0,080581	0,060911	NR1H2,NAPSA
chr6	1,64E+08	1,64E+08	715	6	0,000407	0,001772	-0,09124	-0,06431	AL078602.1
chr12	9217079	9217907	829	11	0,001172	0,002018	-0,10539	-0,06154	LINC00612,A2M-AS1
chr11	396686	397486	801	5	0,000753	0,002831	0,095488	0,070649	PKP3
chr1	1,12E+08	1,12E+08	474	6	0,001355	0,005106	0,063995	0,052387	C1orf162
chr1	47900197	47900327	131	5	0,003204	0,006846	0,079071	0,062555	FOXO2-AS1
chr22	38244746	38244902	157	5	0,001669	0,007427	0,070153	0,055552	ANKRD54,EIF3L
chr2	20441905	20442210	306	5	0,005672	0,007602	0,078123	0,050274	
chr10	1,01E+08	1,01E+08	519	5	0,001764	0,008912	-0,09154	-0,06371	

Start, genomic position of the region's start point; End, genomic position of the region's end point; Width, the width of the region; Stouffer, Stouffer summary transform of the individual CpG false discovery rates (FDRs); Fisher, Fisher combined probability transform of the individual CpG FDRs; Maximum difference: Maximum methylation difference within the DMR; Mean difference: Mean methylation difference across the DMR.

References

1. Menke, L.A., van Belzen, M.J., Alders, M., Cristofoli, F., Ehmke, N., Fergelot, P., Foster, A., Gerkes, E.H., Hoffer, M.J., Horn, D., et al. (2016). CREBBP mutations in individuals without Rubinstein-Taybi syndrome phenotype. *Am J Med Genet A* 170, 2681-2693. 10.1002/ajmg.a.37800.
2. Menke, L.A., Gardeitchik, T., Hammond, P., Heimdal, K.R., Houge, G., Hufnagel, S.B., Ji, J., Johansson, S., Kant, S.G., Kinning, E., et al. (2018). Further delineation of an entity caused by CREBBP and EP300 mutations but not resembling Rubinstein-Taybi syndrome. *Am J Med Genet A* 176, 862-876. 10.1002/ajmg.a.38626.
3. Angius, A., Uva, P., Oppo, M., Persico, I., Onano, S., Olla, S., Pes, V., Perria, C., Cuccuru, G., Atzeni, R., et al. (2019). Confirmation of a new phenotype in an individual with a variant in the last part of exon 30 of CREBBP. *Am J Med Genet A* 179, 634-638. 10.1002/ajmg.a.61052.
4. Banka, S., Sayer, R., Breen, C., Barton, S., Pavaine, J., Sheppard, S.E., Bedoukian, E., Skraban, C., Cuddapah, V.A., and Clayton-Smith, J. (2019). Genotype-phenotype specificity in Menke-Hennekam syndrome caused by missense variants in exon 30 or 31 of CREBBP. *Am J Med Genet A* 179, 1058-1062. 10.1002/ajmg.a.61131.